

## SYNTHESIS AND STRUCTURAL FEATURES OF A FLUX-GROWN HEMATITE

SHU-CHENG YU, JIANN-SHING LEE, SHU-FANG TUNG and CHUI-LONG LAN

Department of Earth Sciences, National Cheng-Kung University, Tainan

### ABSTRACT

Almost pure  $\text{Fe}_2\text{O}_3$  hematite crystals exhibiting a superior metallic luster were produced in an emerald synthesis experiment using a flux-growth process. The grown specular hematites were platy crystals approximately 0.5 mm thick, 10 mm long and 10 mm high, exhibiting apparent twinning boundaries on the crystal surface. The growth was initiated at  $1200^\circ\text{C}$ , in a platinum crucible, followed by a two-stage slow cooling process. The first stage involved cooling from  $1200^\circ\text{C}$  to  $1000^\circ\text{C}$  at a cooling rate of  $0.5^\circ\text{C/h}$ ; the second stage was from  $1000^\circ\text{C}$  to  $900^\circ\text{C}$  at  $1^\circ\text{C/h}$ .

A detailed crystal structure analysis was carried out with two separate synthetic crystals. The structural refinements indicate that the interatomic distances of various bonds are shorter than the corresponding lengths in natural samples. This is a direct consequence of the impurity-free chemical composition of the grown crystals. The most significant structural characteristic in the synthetic hematite is the electron charge distribution surrounding the ferric ion in the octahedral position. The thermal ellipsoid of the  $\text{Fe}^{3+}$  ion is flattened in the (001) plane to form an oblate spheroid. This is in response to the adjacent iron atoms repelling one another along the [001] direction. The dispersed electron charge perpendicular to the c-axis significantly reduces the repelling effect between two adjacent Fe atoms. This stabilizes the otherwise unstable face-sharing octahedral structure.

**Key words:** synthetic hematite, specularite, flux growth, high temperature, crystal structure

## INTRODUCTION

Occurring in various geological environments, hematite is an important iron ore, having played a significant role in the development of the human history ever since the dawn of civilization. In almost every form of construction, transportation, communications and manufacturing, iron is an essential material. It will be as important, or more so, in the coming 21<sup>st</sup> century, and perhaps even further in the future. Hematite occurs chiefly in extensive sedimentary rock formations and as an accessory mineral in igneous and metamorphic rocks. It also occurs in many metamorphic rocks and in contact metamorphic deposits (Roberts *et al.*, 1990). Hematite is also a common cementing material and coloration agent in sandstone formations, especially in redbeds and associated clastic sediments (Zoltai and Stout, 1984).

Because the atom in the hematite crystal is fully oxidized, it adopts a corundum ( $\alpha$ -Al<sub>2</sub>O<sub>3</sub>) type of structure (Bragg *et al.*, 1965; Zoltai and Stout, 1984). Structure of hematite was first analyzed by Pauling and Hendricks (Bragg *et al.*, 1965) and later refined by Blake *et al.* (1966). Oxygen atoms in the hematite structure are stacked in a hexagonal close-packed array, while ferric ions occupy two thirds of the total available octahedral sites with one third of the octahedral voids arranged systematically (Newnham and de Haan, 1962). The larger ionic radius of Fe<sup>3+</sup> compared with Al<sup>3+</sup> results in the Fe-O bond being longer than the Al-O bond. Consequently, many physical properties of hematite crystal, such as hardness and melting point, are inferior to those of the corundum mineral, in spite of their identical structure (Yu, 1987). In contrast to  $\alpha$ -Fe<sub>2</sub>O<sub>3</sub>,  $\gamma$ -Fe<sub>2</sub>O<sub>3</sub> is a mineral maghemite, which has a spinel type of structure (Deer *et al.*, 1992).

Because hematite is relatively abundant, little research has been done on the synthesis of hematite crystals. Most studies on hematite growth have been associated with other aspects, such as equilibrium phase diagrams, crystal chemical analysis at various temperatures and pressures, etc. (e.g., Prewitt *et al.*, 1969). Recently, platy hematite crystals with metallic luster were obtained in our flux-growth experiment for emerald crystals. Preliminary optical examination suggested that they were almost perfect crystals. Detailed chemical analysis and crystal structure determination were then carried out on the synthetic crystals to document their chemical and structural characteristics and compare them with those of natural samples.

## EXPERIMENTAL PROCEDURES

## Synthesis Technique

Platy hematite crystals with a metallic luster (specularite) were produced in a flux-growth experiment, which was supposed to synthesize emerald crystals. The precursor materials included alumina, silica and beryllium oxide powders of reagent grade. These were mixed with a minor amount of coloration agents, chromium oxide and ferric oxide. The powder mixture was then placed in a platinum crucible covered with a platinum lid. The furnace was heated to a temperature slightly over 1200°C with a heating rate of 10°C/h. The nucleation and growth were induced by a two-step slow-cooling process, where the cooling rate was set at 0.5°C/h between 1200°C and 1000°C; and 1°C/h between 1000°C and 900°C. Platy hematites were found on top of the crucible and were mechanically removed for optical examination, chemical composition determination and X-ray diffraction analysis. The hematite crystals were produced only when a 3 wt% (weight percent) of iron oxide powder was added into the precursor mixture.

## Composition and X-ray Analysis

Chemical composition of the flux-grown hematite samples was determined with a JEOL JSM-840A scanning electron microscope (SEM) equipped with an energy dispersive X-ray (EDX) analysis system. SEM was operated at 20 kV of applied voltage and 10 nA of sample current.

Two hematite crystals, approximately 95 x 220 x 250  $\mu$ m and 125 x 180 x 470  $\mu$ m, referred to as Crystals 1 and 2, throughout this paper were selected for single crystal X-ray diffraction analysis. X-ray intensity data were collected on an Enraf-Nonius CAD-4 four circle single crystal diffractometer with MoK $\alpha$  radiation and a  $\omega$ -2 $\theta$  scan mode operation. A total of 1100 reflections were recorded in the 2 $\theta$  range between 10° and 100°, in which about 350 were independent reflections. Structure of Crystal 1 was analyzed and refined with an NRCVAX crystal structure system, and that of Crystal 2 was done with a full-matrix least-squares method of the SHELXTAL program provided by Professor T. J. Lee of National Tsing-hua University. R factor obtained in the final stage of refinement for both crystals was approximately 4%.

## RESULTS AND DISCUSSION

## Basic Crystal Data

EDX analysis results shown in Table 1 indicate that chemical composition of this flux-grown hematite crystal is essentially Fe<sub>2</sub>O<sub>3</sub>. However, the crystal does contain trace amounts of Al<sub>2</sub>O<sub>3</sub>, Cr<sub>2</sub>O<sub>3</sub> and CaO. Calcium oxide is believed to be the result of contamination, as no calcium was added to the precursor mixture. Errors in the analysis are less than 8% for Al and less than 0.7% for Fe. Two slightly varied chemical formulae were then calculated, depending on whether or not Ca atoms were included. They are Fe<sub>1.954</sub>Al<sub>0.042</sub>Cr<sub>0.004</sub>O<sub>3</sub> and Fe<sub>1.950</sub>Al<sub>0.042</sub>Cr<sub>0.004</sub>Ca<sub>0.004</sub>O<sub>3</sub>. The difference in these two chemical formulae is insignificant. As discussed later, excluding the Ca cations from the chemical composition also has a very limited effect on the final result of the crystal structure analysis.

Two sets of unit cell parameters as refined on the CAD-4 diffractometer are listed in Table 2 along with other crystallographic data for the two hematite crystals. From the statistical uncertainty, it is evident that the unit cell constants derived from the two hematite samples are consistent. However, both sets of the cell parameters are shorter than those reported in the literature: a=5.038Å and c=13.772Å (Blake *et al.*, 1966); a=5.0351(3)Å and c=13.750(1) (Prewitt *et al.*, 1969); a=5.0490(9)Å and c=13.7524(18)Å (Donnay, 1978).

Comparison of unit cell dimensions is shown in Table 3. The negative deviations in the unit cell parameters of the synthetic hematite samples are considered to be directly related to the chemical composition. The flux-grown crystals of this study are much closer to the ideal chemical composition of Fe<sub>2</sub>O<sub>3</sub> than the samples reported in the literature. Most natural hematite specimens contain a significant amount of Al, Cr and Ti atoms to form a solid solution series. Some of the fibrous or ocherous hematites may contain several percent of water (Berry *et al.*, 1983). This is consistent with the density computation. The calculated density of our hematite sample is 5.27g/cm<sup>3</sup> compared with the value of 5.25g/cm<sup>3</sup> in the literature (Deer *et al.*, 1992). This density difference reflects the fact that natural hematite samples contained more lighter impurity atoms, such as Al, Ti, V, and Cr, than the synthetic crystals.

Table 1. EDX analysis of flux-grown hematite

Oxide	wt%
Al <sub>2</sub> O <sub>3</sub>	1.34
Cr <sub>2</sub> O <sub>3</sub>	0.19
Fe <sub>2</sub> O <sub>3</sub>	98.52
CaO	0.12
Total	100.17

Table 2. Crystal data for the flux-grown hematite

	Crystal 1	Crystal 2
Size ( $\mu\text{m}$ )	95 x 220 x 250	125 x 180 x 470
Space group	R $\bar{3}c$	R $\bar{3}c$
a(A)	5.0206(24)	5.0230(10)
c(A)	13.7196(13)	13.708(3)
Volume (A <sup>3</sup> )	299.5(1)	299.5(1)
Z	6	6
Density (g/cm <sup>3</sup> )	5.27	5.27
R (%)	5.3	3.9
R <sub>w</sub> (%)	7.6	9.1

Table 3. Unit cell parameters of various hematites

	a(A)	c(A)
Blake et al. (1966)	5.038	13.772
Kastalsky & Westcott (1968)	5.0340(7)	13.752(3)
Prewitt et al. (1969)	5.035(3)	13.750(1)
Donnay (1978)	5.0490(9)	13.7524(18)
Crystal 1*	5.0206(24)	13.7196(13)
Crystal 2*	5.0230(0)	13.708(3)

\* This study

## Anisotropic Charge Distribution

The final atomic coordinates of the synthetic hematite crystals are listed in Table 4. Within the present experimental uncertainty, the atomic positional parameters of Crystals 1 and 2 are regarded as identical. The corresponding isotropic temperature factors (Tab. 4) for the two synthetic samples are also very similar. A slight variation is evident when one looks at the anisotropic thermal parameters in these two crystals, as shown in Table 5. Both the ferric iron and oxygen atoms of Crystal 1 display smaller anisotropic displacement parameters than those of Crystal 2, in spite of the fact that the final R factor for Crystal 1 is slightly greater than that of Crystal 2 (5.3% vs. 3.9%; see Tab. 2). The three principal values of the anisotropic temperature factors for iron and oxygen atoms in the two structural refinements indicate that the thermal ellipsoids are relatively flattened in the (001) plane to form an oblate spheroid, as shown in Figure 1.

	Crystal 1	Crystal 2
<b>Fe</b>		
x	0.0000	0.0000
y	0.0000	0.0000
z	0.35529(6)	0.3553(1)
B	0.37(0)	0.39(8)
<b>O</b>		
x	0.6953(7)	0.6940(2)
y	0.0000	0.0000
z	0.2500	0.2500
B	0.48(8)	0.47(8)

Table 4. Atomic coordinates and equivalent isotropic temperature factors of flux-grown hematite crystals

	Crystal 1	Crystal 2
<b>Fe</b>		
U <sub>11</sub>	56(0)	70(10)
U <sub>22</sub>	56(0)	70(10)
U <sub>33</sub>	29(0)	20(10)
U <sub>12</sub>	28(0)	30(10)
U <sub>23</sub>	0(0)	0(0)
U <sub>13</sub>	0(0)	0(0)
<b>O</b>		
U <sub>11</sub>	64(8)	70(10)
U <sub>22</sub>	64(0)	80(10)
U <sub>33</sub>	48(10)	40(10)
U <sub>12</sub>	28(11)	40(10)
U <sub>23</sub>	2(5)	10(0)
U <sub>13</sub>	-2(0)	0(10)

Table 5. Anisotropic displacement parameters (X10<sup>4</sup>) of flux-grown hematite crystals

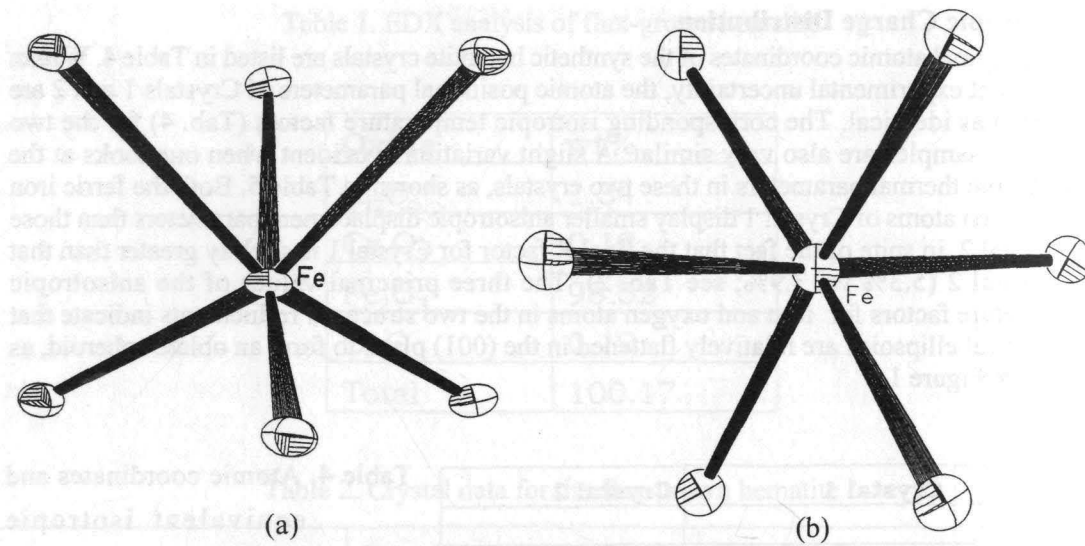


Figure 1. The thermal ellipsoids of the ferric iron and oxygen atoms in the flux-grown hematite crystal projected along the a-axis (a) and along the c-axis (b).

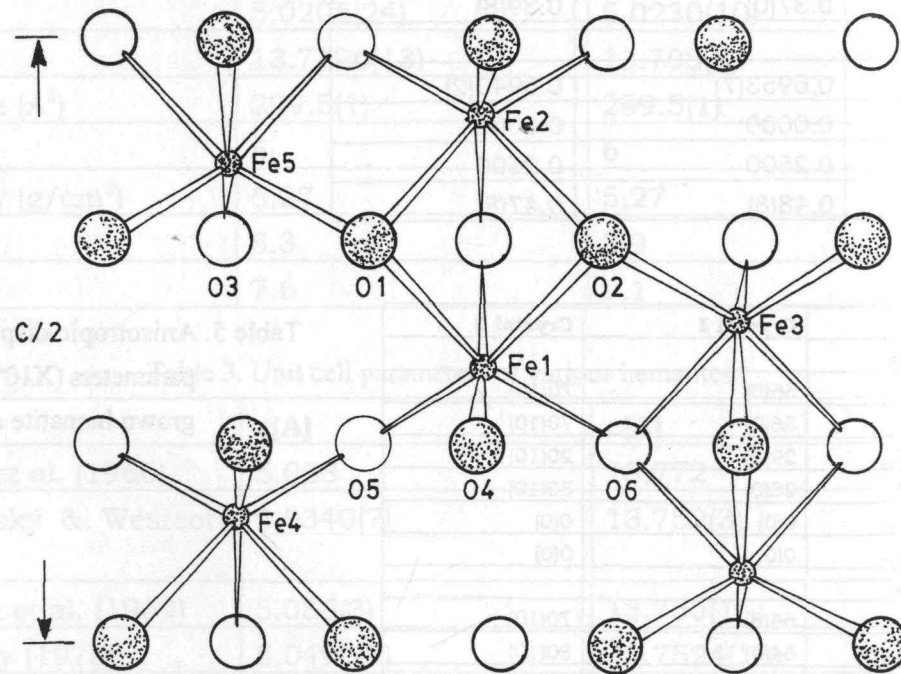


Figure 2. The corundum structure projected along the a-axis of the hexagonal cell (redrawn from Newnham and de Haan, 1962).

Figure 2 shows one of the important structural characteristics in the corundum-type of structure--separation of the two adjacent octahedral cations along the c-axis. This effect is due primarily to the large repellant force resulting from the adjacent octahedra sharing the same face (Newnham and de Haan, 1962). This separation causes the ferric ions in the hematite structure to be off the geometric center of the octahedra formed by oxygen atoms. This cationic displacement can also be understood by looking at the interatomic distance between two adjacent iron atoms, Fe(1) and Fe(2) (Fig. 2). As listed in Table 6, this interatomic distance of 2.886A (literature value 2.900A) is shorter than 2.962A (literature value 2.971A) for the Fe(1)-Fe(3) distance, which is in a direction almost perpendicular to the c-axis (Fig. 2). Consequently, it is expected that the electron charge distribution of the Fe cations disperses in the (001) plane and produces a flattened Fe thermal ellipsoid along the c-axis. This important structural feature of the thermal motion in the octahedral ferric ions was unequivocally demonstrated for the first time in the present structure refinements for both synthetic hematite crystals.

Table 6. Bond distances and bond angles of the flux-grown hematite crystals

Distance(A)	Crystal 1	Crystal 2	Fe <sub>2</sub> O <sub>3</sub> *
Fe(1)-O(1)	2.1068(16)	2.1085(8)	2.116
Fe(1)-O(5)	1.9399(11)	1.9391(6)	1.945
Fe(1)-Fe(2)	2.8866(11)	2.8862(8)	2.900
Fe(1)-Fe(3)	2.9614(8)	2.9618(6)	2.971
Fe(1)-Fe(5)	3.6916(7)	3.6919(6)	3.706
<b>Angle(°)</b>			
O(1)-Fe(1)-O(2)	78.28(4)	78.31(3)	78.2
O(1)-Fe(1)-O(5)	86.03(5)	86.03(1)	86.1
O(5)-Fe(1)-O(6)	102.54(8)	102.56(1)	102.6
O(1)-Fe(1)-O(6)	162.24(6)	162.24(3)	162.4
Fe(1)-O(1)-Fe(2)	86.41(8)	86.38(4)	86.6
Fe(1)-O(2)-Fe(3)	93.97(3)	93.97(1)	94.0
Fe(1)-O(5)-Fe(4)	119.62(10)	119.68(5)	119.7
Fe(1)-O(1)-Fe(5)	131.59(3)	131.56(2)	131.7

\* Blake et al. (1966).

### Fe-octahedral Geometry

Comparison of the bond distances and bond angles of the flux-grown hematite refined from two separate crystals is shown in Table 6 along with the corresponding values from the literature (Blake *et al.*, 1966). The most fundamental structural unit in hematite is its  $\text{FeO}_6$  octahedra. The geometric characteristics of the bond angles in the  $\text{FeO}_6$  octahedra of the two synthetic samples are similar to those reported by Blake *et al.* (1966). However, both sets of the refined bond distances for the two flux-grown crystals are slightly shorter than the previously reported values. For example, the bond distances for Fe(1)-O(1) are 2.1068(16) and 2.1085(8) Å, respectively, for synthetic hematite Crystals 1 and 2; whereas the corresponding distance is 2.116 Å for the natural hematite sample. The Fe(1)-O(5) bond length is 1.9399(11) and 1.9391(6) Å for the synthetic Crystals 1 and 2, compared with 1.945 Å for the natural sample. This difference in bond distance is due primarily to the chemical composition of the synthetic impurity-free hematite crystal, which is much closer to the ideal formula of  $\text{Fe}_2\text{O}_3$ , than the natural counterparts, and to the excellent crystallinity of the synthetic samples.

Because of the face-sharing characteristics of two adjacent  $\text{FeO}_6$  octahedra in the hematite structure, the iron atoms are closer to the oxygen (Fe(1)-O(5)) of the unshared faces, 1.940 Å, than to the oxygen (Fe(1)-O(1)) of the shared faces, 2.107 Å (Crystal 1) and 2.109 Å (Crystal 2). The present structural refinement indicates that this type of distortion in the cation-oxygen chemical bonds in hematite is consistent for both synthetic crystals and natural samples regardless of their chemical impurity.

### CONCLUSION

Specular hematite (specularite) crystals in platy form were produced by a flux-growth method. The nucleation and growth of the synthetic crystals involved a two-stage cooling process. A very slow cooling of  $0.5^\circ\text{C}/\text{h}$  was used in the first stage between  $1200^\circ\text{C}$  and  $1000^\circ\text{C}$ , and a  $1^\circ\text{C}/\text{h}$  cooling rate in the second stage from  $1000^\circ\text{C}$  to  $900^\circ\text{C}$ .

Chemical analysis indicates that the flux-grown hematite crystals were nearly pure  $\text{Fe}_2\text{O}_3$ , and contained an insignificant amount of  $\text{Al}_2\text{O}_3$ ,  $\text{Cr}_2\text{O}_3$  and  $\text{CaO}$ . In contrast, Al, Cr, Ti, and V are common metals substituting for Fe atoms in natural hematite.

Crystal structure determination carried out with two separate synthetic crystals suggests that electron charge distribution of both ferric iron and oxygen atoms exhibited highly anisotropic characteristics. The distorted electron distribution in the (001) plane resulted in the thermal ellipsoids of iron and oxygen atoms which are flattened perpendicular to the c-axis. This structural feature was unequivocally demonstrated in the hematite crystals studied. This distinct pattern in charge distribution provided the hematite structure with a cationic separation between two adjacent ferric ions. This effect substantially reduced the repellant force and consequently stabilized the otherwise unstable face-shared octahedral structure in hematite.

The octahedral bond angles, or the Fe-O coordination geometry, of the synthetic hematite are basically identical to those of natural crystals. However, the flux-grown samples display a marked negative deviation in the Fe-O bond distances compared with their natural counterparts. This difference is reflected in the impurity-free properties of the synthetic hematite samples. The bond distances between iron atoms and oxygen atoms of the unshared and shared faces are equally distorted for both synthetic and natural hematite samples.

### ACKNOWLEDGMENTS

The authors thank Professors H. J. Lo and J. A. Xu for their constructive comments to improve the manuscript.

### REFERENCES

- Berry, L.G., Mason, B. and Dietrich, R.V. (1983) Oxides and hydroxides. In: *Mineralogy: Concepts, Descriptions, Determinations*, Freeman, New York, N.Y.
- Blake, R.L., Hessevick, R.E., Zoltai, T. and Finger, L.W. (1966) Refinement of the hematite structure: *Amer. Mineral.*, **51**, 123-129.
- Bragg, L., Claringbull, G.F. and Taylor, W.H. (1965) Oxides. In: *Crystal Structures of Minerals*, Cornell University Press, Ithaca, N.Y.
- Deer, W.A., Howie, R.A. and Zussman, J. (1992) Oxides: In: *An Introduction to the Rock-Forming Minerals*, 2<sup>nd</sup> ed. Longman Scientific and Technical, Essex, England.
- Donnay, J. D.H. (1978) Hematite. In: *Crystal Data, Determinative Tables*, 3<sup>rd</sup> ed., **4**, NBS and JCPDS, International Center for Diffraction Data.
- Kastalsky, V. and Westcott, M. F. (1968) Accurate unit cell dimensions of hematite ( $\alpha\text{-Fe}_2\text{O}_3$ ): *Aust. J. Chem.*, **21**, 1061-1062.
- Lee, P.L. (1995) The study on growth of emerald crystals from the flux of  $\text{PbO-V}_2\text{O}_5$  system: M.S. thesis, National Cheng Kung University.
- Newnham, R.E. and de Haan, Y.M. (1962) Refinement of the  $\alpha\text{-Al}_2\text{O}_3$ ,  $\text{Ti}_2\text{O}_3$ ,  $\text{V}_2\text{O}_3$  and  $\text{Cr}_2\text{O}_3$  structures: *Z. Krist.*, **117**, 235-237.
- Prewitt, C.T., Shannon, R.D., Rogers, D.B. and Sleight, A.W. (1969) The rare earth oxide-corundum transition and crystal chemistry of oxides having the corundum structure: *Inorg. Chem.*, **8**, 1985-1993.
- Roberts, W.L., Campbell, T.J. and Rapp, G.R., Jr. (1990) Hematite. In: *Encyclopedia of Minerals*, 2<sup>nd</sup> ed. Van Nostrand, New York, N.Y.
- Yu, S. C. (1987) Basic physical properties of crystals (1): In: *Crystal Structures and Properties*, Bo-hi-tung Publishing Co., Taipei. (in Chinese)
- Zoltai, T. and Stout, J.H. (1984) The oxide minerals. In: *Mineralogy: Concepts and Principles*, Burgess Publishing Co., Minneapolis.

## 鏡鐵礦之助熔法合成及結構特徵

余樹楨、李建興、董淑芳、藍錦龍

國立成功大學地球科學系

## 摘要

以助熔法合成祖母綠實驗中，一種閃亮異常、近乎純氧化鐵成份的鏡鐵礦晶體同時結晶出來。所培育鏡鐵礦為0.5毫米厚、10毫米大的片狀晶體；晶面上出現可能是雙晶的條紋狀顯微構造。長晶步驟包含兩階段的冷卻過程：首先自1200°C以每小時0.5°C的速率緩慢冷卻至1000°C，第二階段則以每小時1°C的速率自1000°C冷卻至900°C。

以兩顆合成鏡鐵礦晶體所進行的結構分析結果同時顯示人造鏡鐵礦晶體結構中的鐵氧鍵長均略小於天然赤鐵礦的鐵氧鍵距。本合成鏡鐵礦原子排列中最具特色的是八面體配位鐵離子的電子雲分布。鐵離子的熱振動橢球沿(001)面明顯呈現扁平化偏移，這是反應相鄰兩鐵離子距離太近所產生相互排斥的結果。由於鐵離子外圍電子雲的扁平分布，因此有效減低正電排斥作用，因而使原本不安定的陽離子共面鏡鐵礦結構轉趨於穩固。

關鍵詞：合成赤鐵礦、鏡鐵礦、助融法長晶、高溫、晶體結構